Clones and other interference effects in the evolution of angular-momentum coherent states

P. Rozmej*
Theoretical Physics Department, Institute of Physics, University Maria Curie-Skłodowska, PL 20-031 Lublin, Poland and Institut des Sciences Nucléaires, F 38026 Grenoble Cedex, France

R. Arvieu†
Institut des Sciences Nucléaires, F 38026 Grenoble Cedex, France
(Received 13 January 1998; revised manuscript received 13 July 1998)

The aim of this paper is to present the interference effects that occur during the time evolution of simple angular wave packets (WP's) which can be associated with a diatomic rigid molecule (heteronuclear) or with a quantum rigid body with axial symmetry like a molecule or a nucleus. The time evolution is understood entirely within the framework of fractional revivals discovered by Averbukh and Perelman (Phys. Lett. A **39**, 449 (1989); Usp. Fiz. Nauk **161**, 41 (1991) [Sov. Phys. Usp. **37**, 572 (1991)]), since the energy spectrum is exactly quadratic. Our objectives are to study how these interference effects differ when there is a change of the initial WP. For this purpose we introduce a two-parameter set of angular-momentum coherent states. On the one hand, this set emerges quite naturally from the three-dimensional coherent states of the harmonic oscillator; on the other hand, this set is shown to be built from intelligent spin states. By varying one parameter (η), a scenario of interferences occurs on the sphere at fractional parts of the revival time that strongly depend on η. For $\eta=\pm 1$ the WP, which coincides with a WP found by Mostowski [Phys. Lett. A **56**, 369 (1976)], is a superposition of Bloch [Phys. Rev. **70**, 460 (1946)] or Radcliffe [J. Phys. A **4**, 313 (1971)] states, and clone exactly in time according to a scenario found for the infinite square well in one dimension, and also for a two-dimensional rotor. In the context of intelligent spin states it is also natural to study the evolution by changing η. For $\eta=0$ the WP is called linear, and in time produces a set of rings with axial symmetry over the sphere. The WP's for other values of η are called elliptic, and sets of fractional waves are generated which make a transition between two symmetries. We call these fractional waves ''mutants.'' For specific times a clone is produced that stands among the mutants. Therefore the change in η produces a change in the quantum spread on the sphere. We have also constructed simple coherent states for a symmetric rotor which are applicable to molecules and nuclei. Their time evolution also shows a cloning mechanism for the rational ratio of moments of inertia. For irrational values of this ratio, the scenario of partial revivals completed by Bluhm, Kostelecky, and Tudose [Phys. Lett. A **222**, 220 (1996)] is valid. [S1050-2947(98)04012-8]

PACS number(s): 03.65.Sq

I. INTRODUCTION

In recent years the existence of a generic behavior for the time evolution of simple quantum systems has been found. In Ref. [1], Averbukh and and Perelman indeed discovered a universal scenario of fractional revivals in the long-term evolution of quantum wave packets of a bounded system which goes beyond the correspondence principle. They established this scenario by expanding the bound-state energies relevant to the wave packet up to second order with respect to the mean energy, thus producing a local spectrum that is linear plus quadratic in one quantum number. For a well-concentrated wave packet at the initial time they defined two time constants $T_{\rm cl}$ and $T_{\rm rev}>T_{\rm cl}$, such that the foregoing evolution of the wave packet is predicted as follows: for $0<t<T_{\rm cl}$, the wave packet spreads around a mean trajectory that can be associated with the underlying classical evolution, while for $T_{\rm cl}<t<T_{\rm rev}$ the wave packet interferes with itself in such a way that for fractional times $t=(m/n)\,T_{\rm rev}$ the wave packet is divided into q fractional wave packets. If n is even, $q=n/2$; if not, then $q=n$. The specificity of the system and that of the wave packet determines the shape of the fractional wave packets which are supposed to be spread regularly around the mean trajectory. At time $t=T_{\rm rev}$, the wave packet is rebuilt either identically or only similarly to the original one, depending on the importance of neglected terms that are higher than quadratic. In some very specific cases, the fractional wave packets are clones of the initial one, as studied in the most recent paper [2], and the revival is exact. This scenario has been validated in a most spectacular manner by several authors for a wave packet in a circular orbit of the hydrogen atom [3]; see also Ref. [4], and Ref. [5] for an elliptic orbit. This was extended by Bluhm and Kostelecky [6] to a very long evolution with a demonstration of superrevivals due to the cubic terms. An analytical explanation for the effects caused by cubic terms was found in Ref. [7]. Examples of vibrational wave packets in the anharmonic potential of a simple molecule have also been found since [8,9]. The scenario was thereafter extended to cases where the energy depends on two quantum numbers [10]. A recent synthesis [11] contained most of the references on this topic, while Ref. [12] was devoted to a definition of the experimental wave packets in atomic physics and molecular physics.

*Electronic address: rozmej@tytan.umcs.lublin.pl and rozmej@isnhp1.in2p3.fr
†Electronic address: arvieu@isn.in2p3.fr

The recurrences studied in Refs. [1–12] are all devoted to wave packets, and can be mathematically explained in terms of special Gauss sums. It is necessary to point out that such sums were earlier extensively used in the physical litterature by Berry and Golberg [13], and Berry [14], who studied the full time evolution of the propagator of a nuclear spin with a Hamiltonian of the form $l_z^2/2J$. These authors developed a renormalization theory and discussed the semiclassical limit. More recently [15], various Talbot effects (integer, fractional, fractal) were also discovered with the help of these techniques. Finally Berry [16] showed the occurrence of fractal dimensions both in space and time during the evolution of a uniform wave packet (WP) in boxes of arbitrary dimensions.

Our aim is to consider only angular wave packets for diatomic molecules and also for symmetric rotors, and our purpose is to discuss the time evolution of a large enough set of coherent states of the angular momentum. There is a rather extensive literature on the coherent states. A full bibliography on this subject can be found in Ref. [17]. However, we will focus on the *intelligent spin states* described in Refs. [18–23]. Large efforts have been made to build up such wave packets mainly in the context of group theory. Little effort, on the contrary, has been made to understand their time evolution in detail. Until the work of Ref. [1], it was not realized that they could evolve according to a universal scenario. For a diatomic molecule or for a symmetric rotor, the spectra of which are quadratic in quantum number, such as, for example, the systems discussed in Refs. [2,24], the universal scenario is exact and repeats with period T_{rev}. The main question is whether the fractional wave packets are clones, or just resemble to the initial ones. Despite all efforts to concentrate the wave packet initially in the best possible way, the quantum evolution destroys this concentration (spatial localization) according to the rule formulated in Ref. [1]. In this paper we will show under what conditions the wave packets separate into clones, and in what conditions there is a more restricted scenario of partial revivals. We will also show the existence of fractional waves with different shapes that we call ''mutants.'' It is crucial to present a simple and physically meaningful picture of a coherent state and to decrease the number of its parameters to a minimum. One should keep in mind that a coherent wave packet has a classical content larger than the eigenstates of the angular momentum. Due to this property, it is possible to choose a coherent wave packet in the simplest manner, as we will show below.

In Sec. II we will study a large set of coherent angular WP's which depend only on the angles θ and ϕ. If we impose one condition of minimum uncertainty, these WP's are composed of eigenstates of L^2 and contain, after a proper choice of the axis of coordinates, only spherical harmonics with a magnetic quantum number m of the same parity as l. These states belong to a family of coherent states called *intelligent spin states* [18–23]. The main body of this paper is organized around a particular subset: exponential WP's, which are shown to be narrowly related to the coherent states of the harmonic oscillator (see the Appendix). Moreover the angular spread of the probability density depends on a single adjustable parameter. One of the limiting cases is a WP derived originally by Mostowski [25] for a diatomic molecule, and it is called circular. By varying one parameter one obtains WP's with a cylindrical symmetry, which we call linear, and a large set called elliptic. Each element of this set corresponds to a quantum system like a diatomic molecule or a nucleus in a pure state with a specific preparation, giving it an average angular momentum, an angular distribution, and a particular spread of the distribution of the angular momentum.

In Sec. III it will be shown that a WP obtained by Atkins and Dobson [26], using a Schwinger [27] boson representation of spin $\frac{1}{2}$, is a particular circular state almost coincident with the exponential WP. More generally the boson representation for a spin s is also shown to lead to circular states. The exponential WP provides a closed and compact expression in the angular variables.

In Sec. IV we will state precisely for our angular WP the scenario of fractional revivals derived in Ref. [1] for the general case. It is indeed possible to specify the shape of the fractional revivals. The most spectacular event of cloning, found essentially for an infinite square well in one dimension [2], and for a two-dimensional rotor in Ref. [11], is extended here to the most general case of a circular WP. For linear and elliptic WP's the fractional waves are generally different from the initial WP's due to the quantum spread. However, for a particular set of times, a single clone exists which coincides with the initial WP. In the case of the most general linear WP the fractional waves keep a cylindrical symmetry, showing isotropy in the spread over the sphere. For the elliptic WP the fractional waves should accommodate two limiting symmetries: the plane symmetry present for circular states, and the cylindrical symmetry valid for the linear states. We call these intermediate fractional waves mutants.

In Sec. V we present a numerical calculation showing this evolution for an exponential WP. The cases where cloning occurs is somewhat obvious; however, it is interesting to define properly the time windows during which a given system of clones governs the time evolution. The ''carpet'' representation, used elsewhere [33], is an interesting tool in this respect. A second interesting result of this section lies in the shape of the mutants, which can hardly be found from analytical considerations. It is found that these fractional waves preserve a good angular localization on the sphere. However, their shape differs from that of the initial WP since the generic structure is a well-defined crescentlike shape.

Finally in Sec. VI, we will construct an angular-momentum coherent state of a symmetric rigid rotor according to the rules defined by Janssen [28]. The time evolution of such a state is studied in Sec. VII. Once the number of parameters is reduced, the time evolution of the coherent state, which is now a three-dimensional system with two quantum numbers as in Ref. [10], presents clones if the ratio of the moments of inertia is rational. In the case when this ratio is not a rational number, the fractional wave packets are not clones.

II. DERIVATION OF COHERENT ANGULAR WAVE PACKETS

Coherent angular WP's can be defined as functions of θ and ϕ, which fulfill two requirements.

(1) Their angular spread should be under control, i.e., it should be possible to adjust their angular distribution in the

easiest manner by changing a few parameters or a simple function.

(2) A criterion of minimum uncertainty should be obeyed in a manner similar to the conditions satisfied by the coherent states of the harmonic oscillator:

$$\Delta q_i \, \Delta p_i = \frac{\hbar}{2}, \quad i = x,y,z. \tag{1}$$

In this direction many attempts have used uncertainty relations derived with the angular variables and the angular momentum operator (see, for example, Ref. [17] for a complete reference to these works). Despite the long list of works devoted to this field, there is no detailed description of the time evolution of these WP's in the literature, as we stated in Sec. I. The first attempts in line with modern developments were made in Ref. [11], in which a WP of the rigid rotor in two dimensions was shown to clone exactly. Our work will extend these results to three dimensions, and will discuss a rather large class of WP.

In the following we will use only uncertainty relations based upon the components of the angular momentum and we will call all the states which satisfy

$$\Delta L_x^2 \, \Delta L_y^2 = \tfrac{1}{4} \langle L_z \rangle^2 \tag{2}$$

coherent states. We assume that this equation holds with the axis of coordinates such that

$$\langle L_x \rangle = 0, \quad \langle L_y \rangle = 0. \tag{3}$$

It is a textbook result that a general WP satisfies the inequality (in units with $\hbar = 1$)

$$\Delta L_x^2 \, \Delta L_y^2 \geqslant \tfrac{1}{4} |\langle [L_x, L_y] \rangle|^2. \tag{4}$$

This result is derived by considering the norm of the state obtained by application of a special combination of L_x and L_y, which involve a real parameter called η:

$$(L_x + \mathrm{i} \eta L_y) |\Psi\rangle. \tag{5}$$

If the minimum uncertainty condition is realized, there exists a value of η for which

$$(L_x + \mathrm{i} \eta L_y) |\Psi\rangle = 0. \tag{6}$$

This value of η is related to the average values by two formulas [29]:

$$\eta = \frac{\langle L_z \rangle}{2 \Delta L_y^2} = \pm \sqrt{\frac{\Delta L_x^2}{\Delta L_y^2}}. \tag{7}$$

The second of these equations provides a meaningful interpretation of η in terms of ΔL_x^2 and ΔL_y^2. Let us now construct states which satisfy Eq. (6).

A. Eigenstates of L^2

The simplest and most natural possibility is to construct the states $|\Psi\rangle$ as eigenstates of L^2. This problem was solved long ago [18–23], and the solutions were called *intelligent spin states*. Let us briefly sketch a few of their properties and explain why we will consider only a subset of them.

The intelligent spin states are the eigenstates $|w\rangle$ of L^2 and of the (non-Hermitian) operator $L_x + \mathrm{i} \eta L_y$, with an eigenvalue w such that

$$(L_x + \mathrm{i} \eta L_y) |w\rangle = w |w\rangle. \tag{8}$$

The $2l+1$ eigenvectors of Eq. (8) were discussed extensively in Refs. [19–21]. It was shown by Rashid [21] that there is a one-to-one correspondence between each eigenvector $|w\rangle$ and a parent state $|lm\rangle$. Therefore, instead of $|w\rangle$ it is better to denote a solution of Eq. (8) as $|\eta \, lm\rangle$. The relation between $|lm\rangle$ and $|\eta \, lm\rangle$ implies a normalization factor a_{lm} given in Ref. [21], and an operator such that

$$|w\rangle = |\eta \, lm\rangle = a_{lm} \exp(\delta L_z) \exp\left(-i \frac{\pi}{2} L_y \right) |lm\rangle. \tag{9}$$

The parameter δ is related to η by

$$\exp(\delta) = \sqrt{\frac{1+\eta}{1-\eta}}, \tag{10}$$

and the eigenvalue w is expressed in terms of m by

$$w = m \sqrt{1-\eta^2}. \tag{11}$$

Among the $2l+1$ states [Eq. (9)], one can identify the following.

(1) The states with $m=0$ which fulfill Eqs. (2) and (3). These states will be taken into account, and will be made explicit thereafter.

(2) The states with $m = \pm 1$. These particular states were first introduced by Bloch and Radcliffe [18]. In a more convenient system of coordinates they fulfill the simpler equation with $\eta = 1$ [20,21]:

$$(L_x + \mathrm{i} L_y) |w\rangle = 0. \tag{12}$$

Therefore, these states will also be considered in our paper, and we will call them circular states.

(3) The states for which the parent value m is neither 0 or ± 1. These states do not coincide with the previous ones. However, they are not orthogonal to them. Moreover, they require a value of l larger than or equal to 2, i.e., a tensor of rank at least equal to 2 is needed in order to generate them. We have not studied these states, and it is still an open question of how to build a convenient WP by implying them.

Conversely, the states with $m=0$ can be generated quite naturally starting from a three-dimensional Gaussian WP, as shown in the Appendix, and they require a very simple vector operator. The states with $m=0$ have a very simple structure in terms of spherical harmonics, which is worth briefly presenting independently on grounds of the general solution found in Ref. [21]. Let us denote by $\mathcal{Y}_\eta^l(\theta,\phi)$ these new spherical harmonics which depend on a continuous real parameter η, and let us expand them in terms of the usual Y_m^l as

$$\mathcal{Y}^l_\eta(\theta,\phi)=\sum_{m=-l}^{l} C^l_m(\eta)Y^l_m(\theta,\phi). \tag{13}$$

The recurrence between the C^l_m derived from Eq. (6) implies that sum (13) is restricted in such a way that m and l have the same parity; indeed the recurrence is

$$C^l_{m+1}=-C^l_{m-1}\frac{1+\eta}{1-\eta}\sqrt{\frac{l(l+1)-m(m-1)}{l(l+1)-m(m+1)}}. \tag{14}$$

In the following we will need the expression of $\mathcal{Y}^l_\eta$ for $l=1$, which is

$$\mathcal{Y}^1_\eta(\theta,\phi)=\frac{(1+\eta)Y^1_1-(1-\eta)Y^1_{-1}}{\sqrt{2(1+\eta^2)}}$$
$$=-\frac{1}{4}\sqrt{\frac{3}{\pi}}\frac{1}{\sqrt{1+\eta^2}}\sin\theta(\cos\phi+i\eta\sin\phi). \tag{15}$$

The combination of θ, ϕ, and η given above will be defined as

$$v=\sin\theta(\cos\phi+i\eta\sin\phi). \tag{16}$$

One has

$$\langle\mathcal{Y}^1_\eta|L_z|\mathcal{Y}^1_\eta\rangle=\frac{2\eta}{1+\eta^2}. \tag{17}$$

Similarly, for $l=2$, the coherent states are

$$\mathcal{Y}^2_\eta(\theta,\phi)=[\tfrac{8}{3}(1+\eta^4)+\tfrac{32}{3}\eta^2]^{-1/2}\{(1+\eta)^2Y^2_2$$
$$-\sqrt{\tfrac{2}{3}}(1-\eta^2)Y^2_0+(1-\eta)^2Y^2_{-2}\}, \tag{18}$$

while the average of L_z is

$$\langle\mathcal{Y}^2_\eta|L_z|\mathcal{Y}^2_\eta\rangle=\frac{6\eta(1+\eta^2)}{1+4\eta^2+\eta^4}. \tag{19}$$

It is interesting to point out that $\eta=\pm1$ corresponds to states with $m=\pm l$, while states with $l=0$ are eigenstates of L_x and can be the more simply written as single spherical harmonics of the angle θ' defined as

$$\cos\theta'=\sin\theta\cos\phi, \tag{20}$$

and one has

$$\mathcal{Y}^l_0(\theta,\phi)=Y^l_0(\theta',\phi')=\sum_{m=-l}^{l} C^l_m(0)\;\; Y^l_m(\theta,\phi). \tag{21}$$

The coherent spherical harmonics $\mathcal{Y}^l_\eta(\theta,\phi)$ have no freedom in them, which allows a proper angular localization. It is therefore necessary to consider linear combinations.

B. General WP's

The most general WP solutions of Eq. (6) which fulfill Eq. (2) will be written as

$$|\Psi_\eta\rangle_{\text{general}}=\sum_l \lambda^l_\eta|\mathcal{Y}^l_\eta\rangle. \tag{22}$$

They depend on η, which can be interpreted with the help of Eq. (7), and on weights λ^l which can be determined in order to provide a convenient angular localization. Again there will be states with $\eta=\pm1$ that will be called circular, and others with $\eta=0$ that will be called linear. The WP defined with other values of η will be called elliptic in the following. The justification of this name will be given in the Appendix. In Sec. III many results will be derived for the particular class of WP that will be defined in Sec. II C. Most of them can be seen to apply to the general WP [Eq. (22)].

C. Exponential coherent WP

Among functions that are possible, those that can be expanded in a power series of the variable v defined by Eq. (16) are particularly interesting, because they will contain all the partial waves $\mathcal{Y}^l_\eta$. We have chosen to concentrate on the exponential coherent WP

$$\Psi_\eta(\theta,\phi)=\sqrt{\frac{N}{2\pi\sinh 2N}}\exp[N\sin\theta(\cos\phi+i\eta\sin\phi)], \tag{23}$$

which possess important properties: they fulfill Eq. (2); they have a direct connection to coherent states of the harmonic oscillator (see the Appendix); and, finally, they have a simple geometrical interpretation. Indeed the real parameter N introduced there allows a proper adjustment of the angular spread. The probability density depends only on N and on the angle θ' defined by Eq. (20); the expression is

$$|\Psi_\eta(\theta,\phi)|^2=\frac{N}{2\pi\sinh 2N}e^{2N\cos\theta'}. \tag{24}$$

If we put $\eta=1$ into Eq. (18), we obtain a coherent state defined by Mostowski [25], who wrote it as

$$\Psi_M(\theta,\phi)=C^{-1/2}e^{N(\vec{u}_1+i\vec{u}_2)\cdot\vec{n}}. \tag{25}$$

Here $\vec{u}_1$ and $\vec{u}_2$ are two perpendicular unit vectors [in our case $\vec{u}_1$ is along Ox and $\vec{u}_2$ along Oy, and we have Eq. (3), and $\vec{n}$ is a unit vector in the direction (θ,ϕ)].

The generalization of Eq. (25) with a parameter η has never been considered until now to our knowledge, and the time evolution has never been studied. Let us point out that Eq. (23) can be generalized as

$$\Psi_\eta(\theta,\phi)=C^{-1/2}e^{N(\vec{u}_1+i\eta\vec{u}_2)\cdot\vec{n}}, \tag{26}$$

with arbitrary but perpendicular $\vec{u}_1$ and $\vec{u}_2$. Calling $\vec{u}_3$ a third unit vector perpendicular to $\vec{u}_1$ and $\vec{u}_2$, we will obtain WP's which do not fulfill Eq. (2) but rather

$$\Delta L_1^2\,\Delta L_2^2=\tfrac{1}{4}\langle L_3\rangle^2. \tag{27}$$

Instead of Eq. (3), we would have

$$\langle L_1\rangle = 0, \quad \langle L_2\rangle = 0. \tag{28}$$

The choice of axis made in Eq. (23) considerably simplifies the interpretation and the partial-wave expansion. This expansion will be given in Sec. II D.

It is not difficult to derive that our Ψ_η, defined by Eq. (23), have the following average values and limits for large N:

$$\langle \Psi_\eta | L_z | \Psi_\eta \rangle = \langle L_z \rangle = \eta[N \coth(2N) - \tfrac{1}{2}] \xrightarrow{N\to\infty} \eta[N - \tfrac{1}{2}]. \tag{29}$$

Therefore Eq. (7) implies that

$$\Delta L_y = \langle L_y^2 \rangle = \frac{1}{2}\left[N \coth(2N) - \frac{1}{2}\right] \xrightarrow{N\to\infty} \frac{1}{2}\left[N - \frac{1}{2}\right], \tag{30}$$

$$\Delta L_x = \langle L_x^2 \rangle = \frac{\eta^2}{2}\left[N \coth(2N) - \frac{1}{2}\right] \xrightarrow{N\to\infty} \frac{\eta^2}{2}\left[N - \frac{1}{2}\right]. \tag{31}$$

The average of L_z^2 and the total uncertainty ΔL_η^2 require independent calculations, with the results

$$\langle L_z^2 \rangle = \langle L_y^2 \rangle [1 - 2\eta^2] + \eta^2 N^2, \tag{32}$$

$$\Delta L_\eta^2 = \langle L^2 \rangle - \langle L_z^2 \rangle \xrightarrow{N\to\infty} N - \frac{1}{2} + \eta^2 \frac{N}{2}. \tag{33}$$

D. Partial-wave expansion of the exponential coherent state

We need to distinguish the case with a general value of η from the simpler cases with $\eta = 1$ or 0. (The cases with $\eta = -1$ or negative η are trivially deduced fom cases with positive η by inversing the sense of rotation of the WP.) For $\eta = 1$, i.e., a circular exponential WP, or Mostowski's WP, one has

$$\Psi_M(\theta,\phi) = \Psi_1(\theta,\phi) = \sqrt{\frac{2N}{\sinh 2N}} \sum_{I=0}^{\infty} \frac{(2N)^I}{\sqrt{(2I+1)!}} Y_I^I(\theta,\phi). \tag{34}$$

For $\eta = 0$, i.e., a linear exponential WP, it is found that

$$\Psi_0(\theta,\phi) = \Psi_0(\theta',\phi') = \sqrt{\frac{N}{2\pi \sinh 2N}}\, e^{N\cos\theta'} \tag{35}$$

$$= \sqrt{\frac{2N}{\sinh 2N}} \sum_{I=0}^{\infty} \sqrt{2I+1} \times \sqrt{\frac{\pi}{2N}} I_{I+(1/2)}(N)\, Y_0^I(\theta',\phi'), \tag{36}$$

where $I_{I+(1/2)}(N)$ is a spherical Bessel function of the first kind.

For a general value of η, i.e., an elliptic WP, the argument v can be separated into two parts

$$v = \frac{1+\eta}{2} \sin\theta\, e^{i\phi} + \frac{1-\eta}{2} \sin\theta\, e^{-i\phi}. \tag{37}$$

Then e^{Nv} is calculated as two power series containing products of Y_l^l and $Y_{-l'}^{l'}$. These products are then expanded in terms of Y_M^I as

$$\Psi_\eta(\theta,\phi) = \sum_{IM} b_{IM}(N,\eta)\, Y_M^I(\theta,\phi), \tag{38}$$

with the weights b_{IM} given by

$$b_{IM}(N,\eta) = \sqrt{\frac{2N}{\sinh(2N)}} \sum_{ll'} \frac{(-1)^{l'}[N(1+\eta)]^l [N(1-\eta)]^{l'}}{\sqrt{(2l)!(2l')!}} \frac{\langle ll'00|I0\rangle \langle ll'l-l'|IM\rangle}{\sqrt{2I+1}}. \tag{39}$$

From the discussion made in Sec. II A, b_{IM} is proportional to C_{IM}. The known selection rules of the Clebsh-Gordan coefficients which appear in Eq. (39) assure that M should have the parity of I.

III. COMPARISON WITH COHERENT STATES DEFINED IN TERMS OF BOSONS

In this section we will compare the previous coherent states to another set defined in terms of bosons of spin s. Based on Schwinger's work [27], several angular-momentum coherent states have been constructed which rely upon a boson representation of spin s. The case with $s = \frac{1}{2}$ was first considered in Ref. [30], and studied more extensively by Atkins and Dobson [26]. Mikhailov [31] generalized this case to any spin integer or half-integer. His work was complemented by Gulshani [32]. According to Mikhailov, a coherent state formed with $2s+1$ bosons depends on two complex numbers called α_+ and α_- combined to define other complex constants α_{jm} by

$$\alpha_{jm} = \alpha_+^{j+m} \alpha_-^{j-m} \begin{pmatrix} 2j \\ j-m \end{pmatrix}^{1/2}, \tag{40}$$

for $j = 0, s, 2s, \ldots, ps, \ldots$ and $m = -j, -j+1, \ldots, j-1, j$.

The coherent state, generically called $|\alpha s\rangle$, is expressed by

$$|\alpha s\rangle = \exp\left(-\frac{n^{2s}}{2}\right) \prod_\mu \exp(\alpha_{s\mu} a_\mu^\dagger)\, |0\rangle \tag{41}$$

$$= \exp\left(-\frac{n^{2s}}{2}\right) \sum_{j=0,s,\ldots,ps,\ldots}^{\infty} \sum_{m=-j}^{j} \frac{1}{\sqrt{p!}} \alpha_{jm} |jms\rangle . \tag{42}$$

$|0\rangle$ represents the vacuum, $a_\mu^\dagger$ $(\mu = -s, \ldots, s)$ is a creation operator of a boson of spin s, and the normalization constant depends on α_+ and α_- through

$$n^{2s} = (|\alpha_+|^2 + |\alpha_-|^2)^{2s} = \sum_\mu |\alpha_{s\mu}|^2 . \tag{43}$$

The states $|jms\rangle$ are normalized states of angular momentum j constructed from $a_\mu^\dagger$ (see Mikhailov for the full expressions). Expansion (42) contains integer and half-integer j's for $s = \frac{1}{2}$, reduces to integer j for $s = 1$, even j, for $s = 2$, etc. States (41) and (42) are eigenstates of the annihilation operator $a_\mu^\dagger$ $(\mu = -s \cdots + s)$ with eigenvalue $\alpha_{s\mu}$. Mikhailov also calculated the expectation values of various operators which are expressed in terms of $a_\mu^\dagger$ and a_μ. Due to this technical simplification, calculations of expectation values are easier than the work necessary to obtain formulas (29)–(33) in the case of the coherent state $\Psi_\eta(\theta, \phi)$. It is interesting to compare the properties of the state $|\alpha s\rangle$ to those of the general state defined by Eq. (22) or (23). Since α_{jm} is generally nonzero for all values of j and m, the states $|\alpha s\rangle$ cannot be identified with our elliptic state for which m should be of the same parity as j. Clearly, formulas (40) and (39) are different. At first sight one could think that Eq. (41), which depends on s and on two complex numbers α_+ and α_-, describes an ensemble of WP's larger than ours [Eq. (23)], which depend only on N and η and would therefore apply to a larger variety of physical situations. We will show that, on the contrary, states (41) are a particular set of circular states and do not contain the freedom allowed with the parameter η. Indeed, if α_+ and α_- are both nonzero, states (41) do not fulfill conditions (3). In order to fulfill these conditions it is necessary that either α_+ or α_- should be zero. [In Ref. [31] it was indeed shown that $\langle L_x \rangle \sim \mathrm{Re}(\alpha_+^* \alpha_-)$ and $\langle L_y \rangle \sim \mathrm{Im}(\alpha_+^* \alpha_-)$.] A change of axis leads to $\alpha_{jm} = 0$ except if $m = j$ (if $\alpha_- = 0$) or $m = -j$ (if $\alpha_+ = 0$). The phase of α_+ or α_- can be incorporated into the phase of the states $|j, m = \pm j, s\rangle$. Choosing, for example, $\alpha_- = 0$ and $\alpha_+ = k =$ (real number), the state $|\alpha s\rangle$ is now simply denoted as $|ks\rangle$:

$$|ks\rangle = \exp\left[-\frac{(k^2)^{2s}}{2}\right] \sum_{j=0,s,\ldots,ps,\ldots}^{\infty} \frac{1}{\sqrt{p!}} (k^2)^j |j = ps, m = j, s\rangle \tag{44}$$

$$= \exp\left(-\frac{k^{4s}}{2}\right) \exp[\alpha_{ss} a_s^\dagger] |0\rangle . \tag{45}$$

In Sec. II, it was clear from the compact expression (25) given by Mostowski that the same physical state can be written by introducing three additional angles which are necessary to specify $\vec{u}_1$ and $\vec{u}_2$. The proof that this freedom also exists in the boson representation was given by Mikhailov [31]. By a convenient choice of axis, the state written in Eq. (41) with $2s+1$ bosons and two complex parameters, can be brought to the simple form of Eqs. (44) and (45) with only one boson of spin s with $\mu = s$ and one parameter $\alpha_{ss} = \alpha_+^{2s} = k^{2s}$. Such a choice was also made by Atkins and Dobson [26] for the case $s = \frac{1}{2}$. The matrix elements of the components of $\vec{L}$ given below are a particular case of formulas given in Ref. [26]:

$$\langle ks|L_z|ks\rangle = s\, k^{4s} , \tag{46}$$

$$\langle ks|L_z^2|ks\rangle = s^2 k^{4s}(k^{4s}+1) , \tag{47}$$

$$\langle ks|L_x^2|ks\rangle = \langle ks|L_y^2|ks\rangle = \frac{s}{2} k^{4s} , \tag{48}$$

$$\Delta L_x^2 \, \Delta L_y^2 = \frac{1}{4} \langle L_z \rangle^2 . \tag{49}$$

These formulas, and expansions (44) and (45), compared to formulas (29)–(32), show that $|ks\rangle$ does not coincide exactly with Mostowski's coherent state. For $s = \frac{1}{2}$, Atkins and Dobson proposed to truncate the sum over j in order to take into account only integer values of j. In this process, the state that we will call $|k, \frac{1}{2}\rangle_i$ (i for integer) needs to be normalized properly, and formulas (46)–(48) cease to be valid. Equation (49) still holds because the state is nevertheless a circular state.

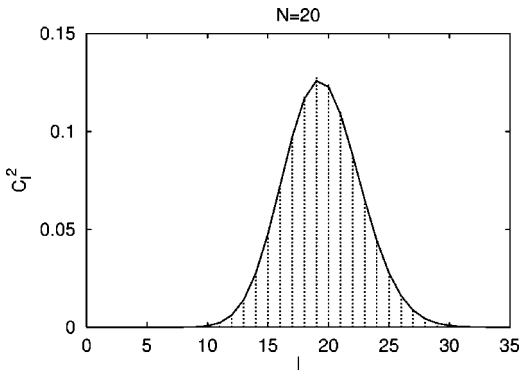

FIG. 1. Probabilities of finding the partial waves Y_l^I in the coherent states of Mostowski (solid line) and Atkins-Dobson (dashed impulses) for parameters $N = 20 = 1/2(k^2+1)$ ensuring the same angular velocity for both wave packets.

Our purpose is now to compare $\Psi_M(\theta,\phi)$ to $|k,\frac{1}{2}\rangle_i$. It is interesting to choose the parameters N and k in such a way that limit (29) for large N is valid ($\eta=1$). Then, using Eq. (46), one puts

$$\tfrac{1}{2}k^2=N-\tfrac{1}{2}. \tag{50}$$

The comparison presented in Fig. 1 shows that the probability C_I^2 of finding the partial wave Y_I^I in Ψ_M and in $|k,\frac{1}{2}\rangle_i$ is practically the same for $N=20$. For smaller N and k (i.e., N of the order of unity) we have observed small but not meaningful differences. It is therefore possible, if N is large enough, to identify Mostowski's coherent state to the boson representation of spin $\frac{1}{2}$ of Atkins and Dobson.

We have shown in this section that the coherent states derived in the literature using a boson representation belong to the particular class of coherent circular states defined in Sec. II. The exponential coherent states defined in Sec. II C above have the advantage of a well-controllable localization, and also depend on an interesting parameter η.

IV. TIME EVOLUTION OF COHERENT ANGULAR WP'S

The coherent states built in Sec. II are applicable to systems which have only angular coordinates on the sphere. This is the case of the three-dimensional rotor with an axis of symmetry like the heteronuclear molecule or some deformed nuclei. In the following we will assume that the eigenvalues of these systems rigorously obey the $I(I+1)$ law, and we will use the frequecy ω_0 written in terms of the moment of inertia J_0 as

$$\omega_0=\frac{\hbar}{2J_0}. \tag{51}$$

Our WP's do not allow us to consider other degrees of freedom such as vibrational or internal excitations. However, we are confident in the usefulness of our work, which provides a full quantum-mechanical description of the rotation of a pure state of a three-dimensional system.

Let us define the *revival time* $T_{\rm rev}$ as

$$T_{\rm rev}=\frac{2\pi}{\omega_0}=(2\overline{I}+1)\,T_{\rm cl}. \tag{52}$$

This time is twice the period of true revival of the WP. Indeed, for the general case (22), one has

$$\Psi_\eta(\theta,\phi,t)_{\rm general}=\sum_I \lambda_I e^{-i2\pi I(I+1)\omega_0 t}\mathcal{Y}_\eta^I(\theta,\phi). \tag{53}$$

Since $I(I+1)$ is always even, the period is indeed $T_{\rm rev}/2$. Nevertheless we will continue to use the same notations as in Ref. [1]. These authors also introduced a second characteristic time $T_{\rm cl}$ called the *classical time*. It is defined in terms of the average angular momentum $\overline{I}$ defined by the average energy of the WP:

$$\overline{I}(\overline{I}+1)=\sum_I |\lambda_I|^2 I(I+1). \tag{54}$$

For the case of an exponential WP, one obtains, with the help of Eqs. (30)–(32),

$$\overline{I}(\overline{I}+1)=\langle L^2\rangle \xrightarrow{N\to\infty} (N-\tfrac{1}{2})+\eta^2[N^2-\tfrac{1}{2}(N-\tfrac{1}{2})]. \tag{55}$$

The classical time $T_{\rm cl}$ is defined as

$$T_{\rm cl}=\frac{2\pi}{\omega_0(2\overline{I}+1)}. \tag{56}$$

$T_{\rm cl}$ is the period of a classical rotator having angular momentum $I=\overline{I}$. At times $t=(m/n)\,T_{\rm rev}$ where $2m<n$ (m and n are mutually prime integers), we will use the trick developed in Ref. [1] to write the quadratic exponential in I as

$$e^{-i\,2\pi I^2(m/n)}=\sum_{s=0}^{l-1} a_s e^{-i2\pi I(s/l)}. \tag{57}$$

It is necessary to distinguish three cases.

(a) n is odd; then $l=n$, and all the coefficients a_s are nonzero. However, they have the same modulus $1/\sqrt{l}$.

(b) n is even and a multiple of 4; then $l=n/2$, and the modulus of a_s has the same value as above.

(c) n is even and not a multiple of 4; then $l=n$, but a_s with even s is zero, and others have their modulus equal to $1/\sqrt{n/2}$.

The number of values of a_s which are nonzero is called q, with $q=n$ if n is odd, and $q=n/2$ if n is even. The phase of a_s can be calculated as described in Ref. [1]. Using these results and inserting Eq. (55) into Eq. (53), one obtains Eqs. (58) and (59) below:

$$\Psi_\eta\left(\theta,\phi,\frac{m}{n}T_{\rm rev}\right)_{\rm general}$$

$$=\sum_I \lambda_I \sum_{s=0}^{l-1} a_s e^{-i2\pi[(m/n)+(s/l)]}\mathcal{Y}_\eta^I(\theta,\phi) \tag{58}$$

$$=\sum_{s=0}^{l-1} a_s \Psi_{\rm cl}^s(\theta,\phi,t_s). \tag{59}$$

At times $t=(m/n)\,T_{\rm rev}$, any WP is a sum of q fractional WP's $\Psi_{\rm cl}^s$, each with a different effective time t_s:

$$t_s=\left(\frac{m}{n}+\frac{s}{l}\right)T_{\rm rev}. \tag{60}$$

The fractional WP at times t_s is given by

$$\Psi_{\rm cl}^s(\theta,\phi,t_s)=\sum_I \lambda_I e^{-iI\omega_0 t_s}\mathcal{Y}_\eta^I(\theta,\phi). \tag{61}$$

There are several cases for which all the $\Psi_{\rm cl}^s$ are clones of the initial WP defined by Eq. (22) for all possible valus of t_s. There are also cases where only one of all the fractional waves is a clone of a particular t_s. Let us describe now these events, keeping arbitrary λ_I in mind as far as possible.

A. Cloning of circular WP's

If $\eta=1$, one has

$$e^{-iI\omega_0 t_s}\mathcal{Y}_1^I(\theta,\phi)=e^{-iI\omega_0 t_s}Y_I^I(\theta,\phi)=Y_I^I(\theta,\phi-\omega_0 t_s). \tag{62}$$

Independently of λ_I, the fractional waves verify the cloning property

$$\Psi_{\rm cl}^{s}(\theta,\phi,t_s)=\Psi(\theta,\phi-\omega_0 t_s,0). \tag{63}$$

Among all circular WP's, which all clone in this way, the exponential WP's, which can be sharply localized in the angle θ by considering high enough N, clone accordingly around q directions disposed symmetrically in the Oxy plane defined by q values of the angle $\omega_0 t_s$.

B. Cloning for some particular t_s

This special situation occurs when there exist values of s such that $\omega_0 t_s$ is a multiple of 2π, and for which a_s is nonzero. Let s_0 be defined by $s_0=n-m$. One has the property

$$\Psi_{\rm cl}^{s_0}(\theta,\phi,t_{s_0})=\Psi(\theta,\phi,0). \tag{64}$$

This event occurs whenever n is odd or even, and not a multiple of 4. The clone is always identical to the initial WP. Obviously it is multiplied by a_{s_0}. The existence of the clone is independent of λ_I and η. For the values of $s\neq s_0$, the fractional WP's are different from the initial WP's. Starting from $\eta=1$ their shape evolves with η, and we propose to call them *mutants*. This *mutation* can indeed be seen as a transition between two symmetries, as we will show numerically in Sec. V.

C. Symmetry properties of the fractional waves

In the following discussion it will be assumed that $\lambda_I\neq 0$ both for even and odd values of I. If some further symmetry is assumed (for example, $\lambda_I=0$ for odd I), properties will result which will not be discussed in the present paper. We first remark that, apart for the value s_0 defined above, associated with a clone, the fractional waves can be paired for each value of m and n in the following manner: associated with s, there exists another value s' such that

$$e^{+iI\omega_0 t_{s'}}=e^{-iI\omega_0 t_s}, \tag{65}$$

and also (noting a difference in the sign of η on the right-hand side)

$$\Psi_{\rm cl}^{s'}(\theta,\phi,t_{s'})_\eta=\Psi_{\rm cl}^{s}(\theta,\phi,t_s)^*_{-\eta}. \tag{66}$$

This equation shows that fractional waves corresponding to opposite η, i.e., opposite $\langle L_z\rangle$, are intermixed. Equality (66) is based on the equality which defines s' in terms of s

$$\frac{t_s+t_{s'}}{T_{\rm rev}}=0 \pmod 1, \tag{67}$$

on the one hand, and from the conjugation property

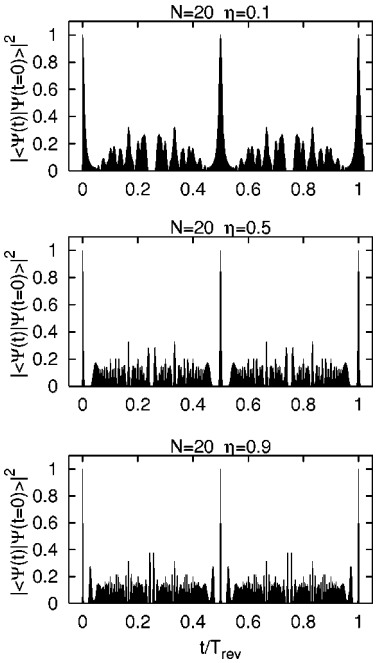

FIG. 2. The autocorrelation function for $N=20$, and different values of parameter η corresponding to a smooth transition between two different symmetries.

$$\mathcal{Y}_\eta^I(\theta,\phi)=\mathcal{Y}^I_{-\eta}{}^*(\theta,\phi) \tag{68}$$

on the other hand. In addition to being real, it is important that λ_I should be an even function of η [as for the exponential WP defined by Eqs. (38) and (39)].

For $\eta=0$ the fractional waves $\Psi_{\rm cl}^{s}$ and $\Psi_{\rm cl}^{s'}$ have the same probability density on the sphere. This leads to a reduction in the number of fractional waves which occur: for odd n, there will be one clone plus $(n-1)/2$ fractional waves; for even n, not a multiple of 4, there is one clone and $(n-2)/4$ fractional waves; finally for n tht is multiple of 4 there will be $n/4$ fractional waves.

V. NUMERICAL CALCULATIONS WITH EXPONENTIAL WP'S

In this section we will describe some figures showing the time evolution of typical exponential coherent WP's. The value of N will generally be the same, and we will change the parameter η. Most of the figures are calculated for $N=20$. This value is typical of rather concentrated WP's. Values near unity correspond to broad WP's which occupy the whole of the sphere and are not interesting for our purpose. Let us note that keeping the same N and changing η produces the same probability density [Eq. (24)] at $t=0$; however, formulas (38)–(39) show that the distribution of the partial wave depends strongly on η. The average $\overline{I}$ is very low for $\eta=0$, and this produce a difference in the time evolution which shows less structure if $N=20$ and if η is decreased. These features can be seen if one studies the autocorrelation function represented for three values of η in Fig. 2. It is seen that this function is composed of peaks which have a larger width if η is small. The structure becomes very

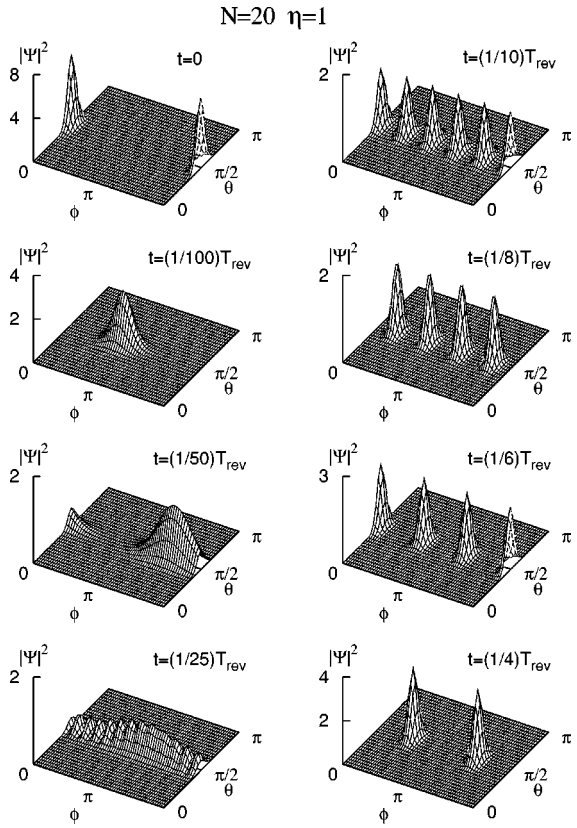

FIG. 3. Time evolution of Mostowski's wave packet with $N=20$. The left column represents changes of the probability density during short term evolution, the right one at fractional revival times. The probability density at times equal 1/5, 1/3, and $1/2*T_{\mathrm{rev}}$ are identical with those presented at 1/10, 1/6, and $1/4*T_{\mathrm{rev}}$, respectively. (The vertical scale is not the same in all figures.)

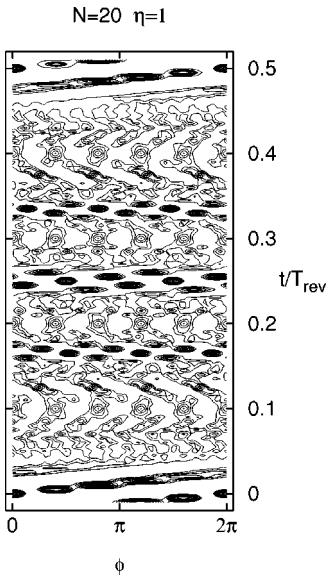

FIG. 4. Time evolution of Mostowski's wave packet with $N=20$. $|\Psi_M(\theta,\phi,t)|^2$ for fixed $\theta=\pi/2$ is presented in the contour plot. The larger values of $|\Psi_M(\theta,\phi,t)|^2$ result in heavy lines due to almost overlapping cuts for fractional revivals. One can clearly see the fractional revivals of orders $\frac{1}{7}$, $\frac{1}{12}$, $\frac{1}{5}$, $\frac{1}{8}$, $\frac{1}{6}$, $\frac{1}{4}$, and so on (corresponding times are $\frac{1}{7}$, $\frac{1}{6}$, $\frac{1}{5}$, $\frac{1}{4}$, $\frac{1}{3}$, and $\frac{1}{2}$ of T_{rev}).

rich if η is nearer to 1. This autocorrelation function is very similar to that studied in Ref. [24].

A. Cloning for circular WP's

The time evolution of the circular wave packet corresponding to $N=20$ is shown in Figs. 3 and 4. In Fig. 3, a convenient set of times has been chosen to show the probability density as a function of θ and ϕ during the regime when the wave packet is spread ($t<T_{\mathrm{cl}}$), then for a few cloning times followed by a full revival for $t=T_{\mathrm{rev}}/2$. In Fig. 4, a ''carpet'' is shown of the section $0\leqslant t\leqslant T_{\mathrm{rev}}/2$ of the probability density for $\theta=\pi/2$, which shows up to $q=7$ clones.

The difference between Mostowski's coherent state and that created by Atkins and Dobson $|k,s=\frac{1}{2}\rangle_i$ is so tiny that it does not present enough interest to be shown. Despite the analogy with the one-dimensional results of the infinite square well [2] and the two-dimensional rotor [11], some interesting aspects of our results need to be stressed. Indeed, circular WP's spread in the ϕ direction and clone around the Oxy plane, which is natural since there is initially a linear momentum along Oy. However, there is no change in time in the azimuthal spread. The cloning mechanism found in quantum mechanics is not possible for a single classical particle; however, it will appear if one uses the ensemble interpretation of quantum mechanics as underlined by authors of Ref. [4].

B. Linear WP's

For $\eta=0$ the fractional WP has cylindrical symmetry around Ox at all times, since it is written as

$$\Psi_{\mathrm{cl}}(\theta',\phi',t)=\sum_I b_I e^{-2i\pi I\, t/T_{\mathrm{rev}}} Y_0^I(\theta',\phi'). \qquad (69)$$

The quantity $2\pi\sin\theta'|\Psi_{\mathrm{cl}}|^2$ is represented in Fig. 5. This shows that the revival wave packets are rings on the sphere and, due to this special topology, do not clone the initial wave function.

The time evolution of $\Psi_0(\theta',\phi',t)$ is represented in Fig. 6. Since the wave packet is in fact one dimensional, the carpet representation provides the essential features of the time evolution. However, in order to produce a similar richness as for $\eta=1$ (and a similar expectation value of L^2), we have increased the value of N for $\eta=0$ to $N=50$. On a sphere, areas of constant probability density could be represented by parallel circles centered on the Ox axis. The pattern of the carpet shown in Fig. 6 very much resembles that

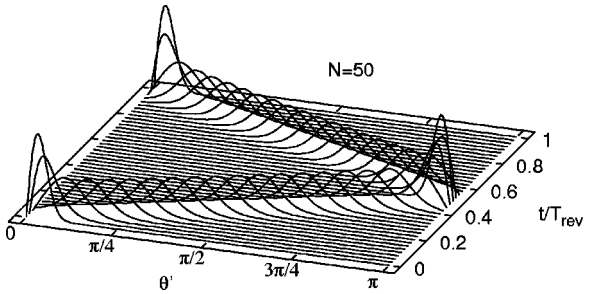

FIG. 5. Time evolution of Ψ_{cl} [Eq. (69)] for $N=50$. The probability density $2\pi\sin\theta'|\Psi_{\mathrm{cl}}|^2$ is presented as a function of θ' and t within one revival period.

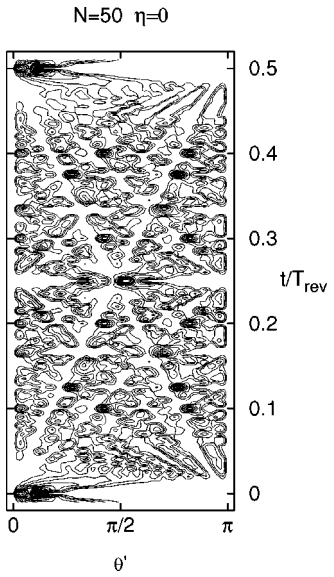

FIG. 6. Time evolution of the wave packet [Eqs. (35) and (36)] for $N=50$. The probability density $2\pi \sin\theta' |\Psi|^2$ is presented in the contour plot. The larger values of $2\pi \sin\theta' |\Psi|^2$ result in heavy lines due to almost overlapping cuts for fractional revivals.

discussed recently in Ref. [33] for a special wave packet in a one-dimensional box. Indeed there is a superposition of ridges and valleys with simple slopes as a function of t. The interpretation of this effect can be given in terms similar to those in Ref. [33]. Note that the quantity plotted in Figs. 6 and 5 has the same boundary conditions as the wave packet on the edge of the box. This produces a reflection effect in Fig. 6 totally absent in Fig. 4, since the boundary conditions are different on the circle. Thus for $\eta=0$ the WP spreads uniformly in all directions defined by the angle ϕ'. Such a WP is total nonsense for a single classical particle, and makes sense only with the ensemble interpretation.

Another interesting linear WP corresponding to $\eta\to\infty$ but keeping ηN finite is defined as follows:

$$\Psi_{\eta N}(\theta,\phi)=\frac{1}{\sqrt{4\pi}}e^{i\eta N\sin\theta\sin\phi}. \tag{70}$$

It is derived from the harmonic oscillator WP of the Appendix by keeping only the term in p_y. This WP has its probability density uniformly distributed over the sphere, and obeys the equation

$$L_y\Psi_{\eta N}=0. \tag{71}$$

It has therefore cylindrical symmetry around Oy, and depends on the angle θ'' defined by

$$\cos\theta''=\sin\theta\sin\phi. \tag{72}$$

Its expansion in spherical harmonics now contains spherical Bessel functions

$$\Psi_{\eta N}=\sum_l \sqrt{2l+1}\, j_l(\eta N)\, Y_0^l(\theta'',\phi''). \tag{73}$$

Obviously the fractional waves also have cylindrical symmetry around Oy, but there is, in addition, for $t=t_{s_0}$, a uniform

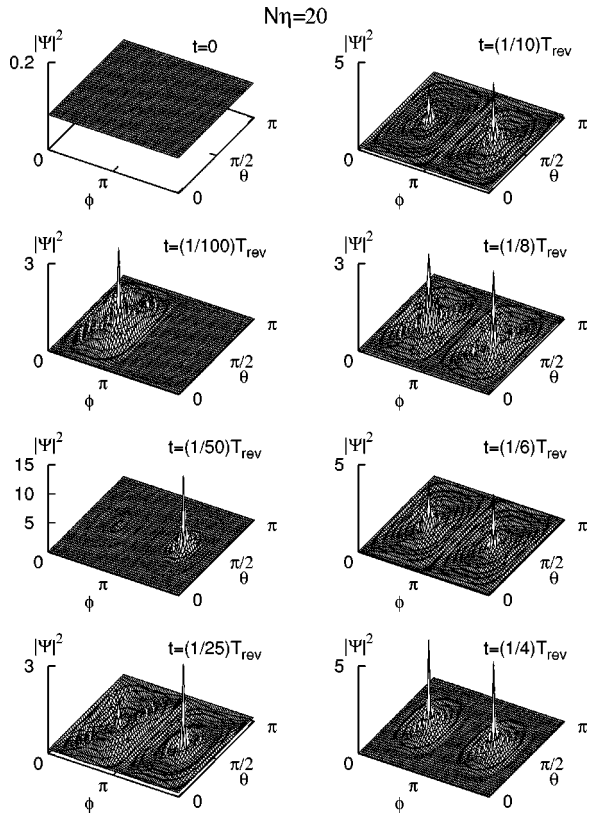

FIG. 7. Time evolution of the WP (70) with infinite η but $\eta N=20$. At $t=0$ the probability density is $1/4\pi$. See explanations in the text.

clone which interferes with all the other fractional waves. The time evolution is shown in Fig. 7 for $\eta N=20$. For small values of t, such as $t=1/100\,T_{\rm rev}$, the WP is concentrated almost totally on the hemisphere with $y>0$, with a spike along Oy surrounded by concentric rings. For $t=1/50\,T_{\rm rev}$ the same behavior occurs, but this time on the hemisphere with $y<0$. For other times both parts of the sphere are covered with rings, and the spike also occurs on both sides of the Oy axis. For $t=T_{\rm rev}\,m/n$, with small m/n, a symmetry between the two hemispheres takes place. The existence of the clone can be seen clearly as a small uniform background at times $t=\frac{1}{25}\,T_{\rm rev}$ and $t=\frac{1}{10}\,T_{\rm rev}$. There is always a strong interference between the fractional waves which does not allow one to make a clear counting even for small values of m/n.

C. Elliptic WP's

For the general elliptic wave packet, as deduced from the previous discussion, there are no clones, but partial revivals with different topology. Due to the change of symmetry, it is indeed necessary to make a smooth transition between a system of clones located for $\eta=1$ in the Oxy plane and the system of rings discussed in Sec. II B. In the system of coordinates adopted in Sec. II A and corresponding to $\eta=0$, these rings have Ox as the symmetry axis. The transition from the clones for $\eta=1$ to the rings for $\eta=0$ is made by developing, for η smaller than 1, a system of pairs of crescents perpendicular to the Oxy plane. This transition is clearly visible in Fig. 8 for particular fractional revival times.

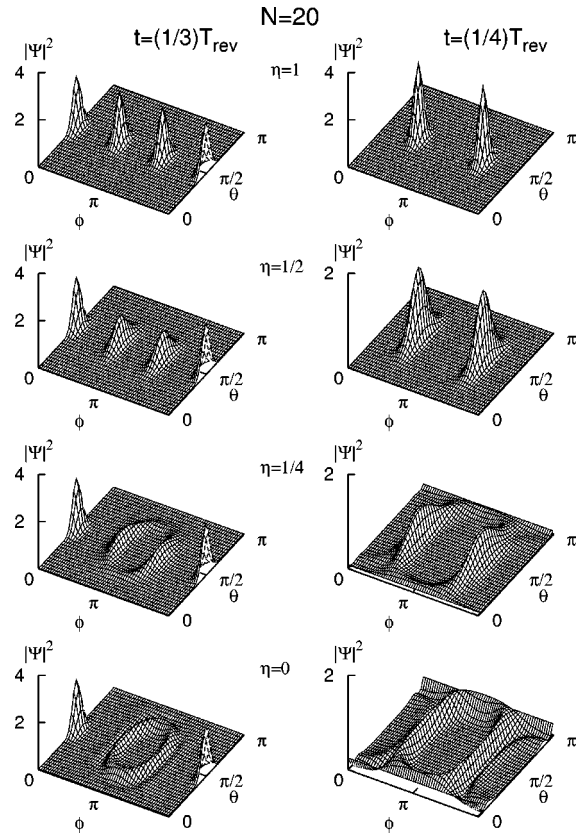

FIG. 8. Transition of fractional wave packets from exact clones ($\eta=1$) through developing crescents ($\eta=1/2, \eta=1/4$) to ring topology ($\eta=0$) is demonstrated for two fractional revival times $t=1/3*T_{\rm rev}$ (left) and $t=1/4*T_{\rm rev}$ (right). The fractional waves called mutants are clearly seen in the lower rows of the figure.

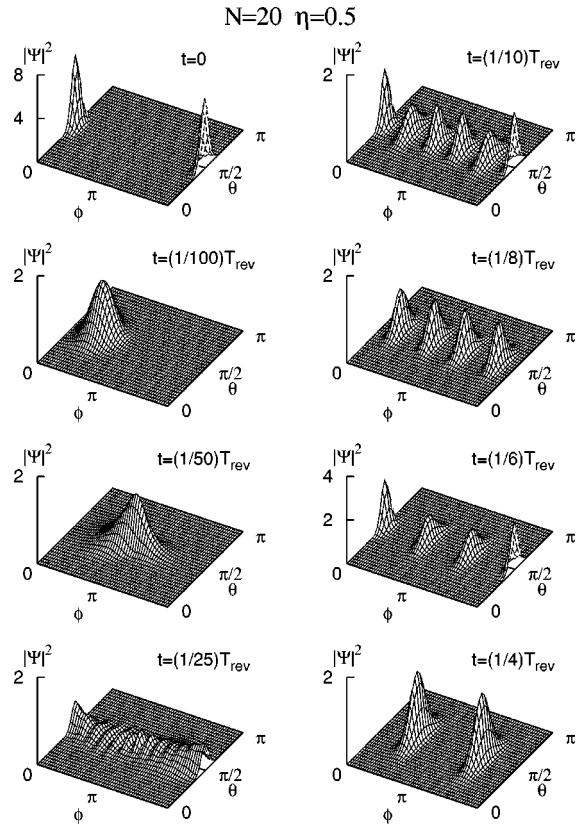

FIG. 9. Time evolution of the coherent state deduced from elliptic motion ($\eta=0.5$). The time sequence presented here is the same as in Fig. 3. Comparing to this figure the crescents are clearly visible; they are the most pronounced for $t=\frac{1}{4}T_{\rm rev}$.

For a very small value of η the upper and lower parts of one crescent meet the corresponding parts of a symmetric crescent in order to build up such a ring symmetric around Ox. Again, this change of topology in the construction forbids the cloning of all fractional waves. Most of them revive in shapes different from that of the initial wave packet. We propose to call these fractional wave packets mutants. An example of the time evolution of wave packet with $\eta=0.5$ is given in Fig. 9. It can be seen in both Figs. 8 and 9 that clones and mutants can occur at the same time. For example, for $\eta=\frac{1}{4}$ and $t=\frac{1}{3}T_{\rm rev}$ there is a fractional revival at $\theta=\pi/2$ and $\phi=0$, with the same shape as the initial wave packet and two crescents which almost close. This situation is similar to that which exists for $\eta=0$ and for $t=\frac{1}{3}T_{\rm rev}$. For $\eta=\frac{1}{2}$ and $t=\frac{1}{6}T_{\rm rev}$, the two crescents do not form a ring. Among the three fractional waves which are present, there are two which are identical to each other but with a larger spread in θ. For this value $\eta=\frac{1}{2}$, there are three different topologies for the five fractional waves. In other publications on a different system [34], we already found a transition from a Gaussian three-dimensional wave packet to a vortex ring. Reference [34] was devoted, as our previous works, to the time evolution of such coherent waves in the case where the Hamiltonian contains a spin-orbit interaction in addition to the harmonic-oscillator potential. If the spin is oriented along the initial wave-packet displacement (Ox axis), the cylindrical symmetry is imposed on the system and preserved during evolution, and vortex rings appear.

The transition between the two shapes of fractional wave packets can be explained by comparing, as a function of η, the spread of the angle θ to the spread of the angle ϕ. If $\eta=0$, the wave packet has no privileged direction on the sphere. It therefore spreads equally. In the case when $\eta=1$, the wave packet is peaked near the plane with $\theta=\pi/2$, and the spread in θ is strongly reduced. The spread in ϕ is seen in the scenario of cloning in the xOy plane. For intermediate values of η, there is a competition between the two effects which manifests itself most strongly in the shape of the fractional waves.

For $\eta>1$ (results not presented), we observed a strong reduction of the spread in θ. For particular values of (m/n), some mutants can be peaked with higher amplitudes than their neighbors. This is in direct connection to the increase in p_0 which was necessary in the initial wave packet.

D. Final remarks

We can measure the aperture of the probability density of the WP by the solid angle $\Omega=4\pi/(4N+1)$ corresponding to the cone defined by $\tan(\theta'/2)=1/2\sqrt{N}$. The time of spreading τ_η of this wave packet of width ΔL_η [Eq. (33)] is of the order of

$$\tau_\eta=\frac{2\pi}{\omega_0}\ \frac{1}{\Delta L_\eta}. \tag{74}$$

The difference in spreading with η is clearly seen in the

autocorrelation functions represented in Fig. 2. We can also define the maximum number of fractional wave packets that can be observed, knowing that $\tan(\theta'/2)=1/2\sqrt{N}$, as

$$q_{\max}=\frac{\pi}{\arctan(1/2\sqrt{N})}. \tag{75}$$

This number is confirmed by the observation of the carpet of Fig. 4 for $N=20$, for which we have up to seven clones. The lifetime τ'_η of a system of q fractional wave packets can be estimated as

$$\omega_0\tau'_\eta\Delta L_\eta=\frac{2\pi}{q}. \tag{76}$$

Also, in Fig. 4, one clearly sees, for $q=2$ and 3, large intervals of time during which clones are observed.

VI. COHERENT STATES FOR A SYMMETRIC TOP

It is natural to enlarge our previous study to include rotational coherent states of symmetric tops which contain an additional degree of freedom. There are several possibilities in the literature for constructing such a state. Our aim is again to choose an axis of coordinates in order to eliminate irrelevant parameters and to make evolution understandable. This is possible only in the case of a symmetric top. We will assume moments of inertia in the intrinsic frame $J_x=J_y$, and introduce the parameter δ such that

$$\delta=\frac{J_x}{J_z}-1. \tag{77}$$

The energy spectrum is then

$$E(I,K)=\frac{\hbar^2}{2J_x}[I(I+1)+\delta K^2]. \tag{78}$$

A convenient rotational wave packet was defined and studied by Janssen [28] on the basis of the work of Perelomov [35] and Schwinger [27]. This wave packet, denoted by three complex numbers x,y, and z, is a mixture of D^I_{MK} functions

$$|xyz\rangle=\exp\left(-\frac{1}{2}yy^*(1+xx^*)(1+zz^*)\right)\times\sum_{IMK}\sqrt{\frac{(2I)!}{(I+M)!(I-M)!(I+K)!(I-K)!}}\times x^{I+M}y^{2I}z^{I+K}|IMK\rangle. \tag{79}$$

The sum over I contains integer as well as half-integer values of I, i.e., this state extends that presented by Atkins and Dobson. Similarly to Sec. III, we call $|xyz\rangle_i$ the normalized projection into space with integer I. A particularly convenient choice of x,y, and z, as well as of the system of coordinates, decreases the number of parameters to two, and reduces the summation to I and K only. The simpler wave packet is then

$$|r,\lambda\rangle=\exp(-r)\sum_{IK}(-1)^{I+K}(2r)^I\frac{\left(\sin\frac{\lambda}{2}\right)^{I+K}\left(\cos\frac{\lambda}{2}\right)^{I-K}}{\sqrt{(I+K)!(I-K)!}}|I-IK\rangle. \tag{80}$$

If L_X, L_Y, and L_Z are the components of $\vec{L}$ in the intrinsic axes L_x, L_y, and L_z, those related to the laboratory axes, one has, according to Janssen,

$$\langle r\lambda|L_x|r\lambda\rangle=\langle r\lambda|L_y|r\lambda\rangle=0,\quad \langle r\lambda|L_z|r\lambda\rangle=-r, \tag{81}$$

$$\langle r\lambda|L_Z|r\lambda\rangle=-r\cos\lambda, \tag{82}$$

$$\langle r\lambda|L_X|r\lambda\rangle=-r\sin\lambda,\quad \langle r\lambda|L_Y|r\lambda\rangle=0,$$

$$\langle r\lambda|L^2|r\lambda\rangle=r(r+\tfrac{3}{2}). \tag{83}$$

Since the WP given by Eq. (80) contains only components with $M=-I$, it is a circular WP with $\eta=-1$ which fulfills Eq. (2) with the components of $\vec{L}$ taken in the laboratory system. From Janssen's work, the components in the rigid-body system verify the equation

$$\Delta L_X^2=\Delta L_Y^2, \tag{84}$$

while their product takes the value

$$\Delta L_X^2\,\Delta L_Y^2=\frac{\langle L_Z\rangle^2}{4\cos^2\lambda}. \tag{85}$$

Therefore, Eq. (2) is also verified for the components in the rigid-body system if OZ is directed along $\vec{L}$. On the other hand, expansion (80) of the rotational coherent states, in terms of $|I-IK\rangle$ has the same coefficients as the expansion of Atkins and Dobson in terms of angular-momentum eigenstates $|IK\rangle$. The two expansions are connected by defining α_+ and α_- as

$$\alpha_+=\sqrt{2r}\sin\frac{\lambda}{2},\quad \alpha_-=\sqrt{2r}\cos\frac{\lambda}{2}. \tag{86}$$

The projection $|r,\lambda\rangle_i$, deduced by restricting Eq. (80) to integer values of I and K, verifies Eqs. (81)–(83) only approximately. However, if r is large enough, these equations are obtained in a very good approximation. The time evolution of the wave packet $|r,\lambda\rangle_i$ will be studied in Sec. VII for a rigid-body symmetric rotor.

VII. TIME EVOLUTION OF JANSSEN'S COHERENT STATE

The energy spectrum of the axially symmetric rigid rotor is written as

$$E_{IK}=\hbar\omega_0[I(I+1)+\delta K^2]. \tag{87}$$

We will study the time evolution of a wave packet deduced from Eq. (80) with $\omega_0=\hbar/(2J_x)$, and with average values

$$\langle r\lambda|L_Z|r\lambda\rangle=\overline{K}=-r\cos\lambda, \tag{88}$$

$$\langle r\lambda|L_z|r\lambda\rangle=\overline{I}=-r. \tag{89}$$

The energy E_{IK} is written by taking $\overline{K}$ and $\overline{I}$ as references, and defining k_1 and k_2 as

$$k_1=I-\overline{I},\quad k_2=K-\overline{K}, \tag{90}$$

$$E_{k_1k_2}=\hbar\omega_0[\overline{I}(\overline{I}+1)+\delta\overline{K}^2]+\hbar\omega_0(2\overline{I}+1)k_1 + \hbar\omega_0\,\delta(2\overline{K})k_2+\hbar\omega_0\,k_1^2+\hbar\omega_0\,\delta k_2^2. \tag{91}$$

We now follow the lines drawn by Bluhm, Kostelecky, and Tudose [10], who considered the time evolution of a system which depends quadratically on two quantum numbers, in our case I and K. There are four time constants: the first pair, defined as

$$T^I_{\rm cl}=\frac{2\pi}{\omega_0(2\overline{I}+1)},\quad T^I_{\rm rev}=\frac{2\pi}{\omega_0}=(2\overline{I}+1)\,T^I_{\rm cl}, \tag{92}$$

is related to the motion around the Oz axis (laboratory axis), i.e., it is connected to the Euler angle α. The second pair plays a parallel role; it concerns the motion around the symmetric OZ axis and the Euler angle γ:

$$T^K_{\rm cl}=\frac{2\pi}{\omega_0\delta 2\overline{K}}=\frac{1}{\delta}\frac{2\overline{I}+1}{2\overline{K}}T^I_{\rm cl},\quad T^K_{\rm rev}=\frac{2\pi}{\delta\omega_0}=\frac{1}{\delta}T^I_{\rm rev}. \tag{93}$$

The system of coordinates and the parametrization in Eq. (80) enable one to profit by the separation of variables in the state $|I-IK\rangle$, since

$$\langle\alpha\beta\gamma|I-IK\rangle=e^{i\alpha I}\,d^I_{-IK}(\beta)\,e^{-i\gamma K}=D^I_{-IK}(\alpha,\beta,\gamma). \tag{94}$$

The wave packet [Eq. (80)] at time t, under conditions (88) and (89) with integers I and K, will be denoted as $|\overline{I\,K}\rangle$ and written as

$$\langle\alpha\beta\gamma|\overline{I\,K}\rangle_t=\sum_{IK}C_{IK}(r,\lambda)\,d^I_{-IK}(\beta)\exp\{i[\alpha I-2\pi I(I+1)\,t/T^I_{\rm rev}]\}\exp[-i(\gamma K+2\pi K^2\,t/T^K_{\rm rev})] \tag{95}$$

$$=\exp\{-i[\overline{I}(\overline{I}+1)+\delta\overline{K}^2]\,t/T^I_{\rm rev}\}\sum_{k_1k_2}C_{k_1k_2}(r,\lambda)\,d^I_{k_1k_2}(\beta)\exp\{i[\alpha k_1-2\pi(k_1/T^I_{\rm cl}+k_1^2/T^I_{\rm rev})t]\} \times\exp\{-i[\gamma k_2+2\pi(k_2/T^K_{\rm cl}+k_2^2/T^K_{\rm rev})t]\}. \tag{96}$$

The summation on I and K has been changed to a sum over k_1 and k_2, and the coefficient $C_{IK}\,d^I_{-IK}$ has been given the new indexes. The discussion of the time evolution of Eqs. (95) and (96) follows that given by Bluhm, Kostelecky, and Tudose [10] in a straightforward manner. The crucial parameter is δ. If $T^K_{\rm rev}$ and $T^I_{\rm rev}$ are not commensurate there is no cloning; however, for $t=(m/n)T^I_{\rm rev}$ there are partial revivals in the variable α: i.e., the wave packet is a superposition of q fractional wave packets peaked regularly along the Oz axis. [$q=(n/2)$ if n is even and n in other cases.] For $t=(m'/n')T^K_{\rm rev}$ the same scenario of partial revival occurs, but this time there are q' fractional wave packets peaked around the OZ axis. [$q'=(n'/2)$ if n' is even, and n' otherwise.]

The interesting situation of commensurability of $T^I_{\rm rev}$ and $T^K_{\rm rev}$ allows, on the contrary, the construction of q^2 clones for all time such that

$$t=\frac{m}{n}T^{I,K}_{\rm rev}. \tag{97}$$

The revival time $T^{I,K}_{\rm rev}$ is the least common multiple of $T^I_{\rm rev}$ and $T^K_{\rm rev}$:

$$p\,T^I_{\rm rev}=r\,T^K_{\rm rev}=T^{I,K}_{\rm rev}. \tag{98}$$

The time evolution of the rotational wave packets is presented in Figs. 10 and 11.

The particular choice $\overline{K}=0$ leads to $T^K_{\rm cl}=\infty$, but $T^K_{\rm rev}$ is finite as well as $T^I_{\rm cl}$ and $T^I_{\rm rev}$. For a smaller value of t, the behavior of the wave packet around Oz and OZ is different, as seen from Fig. 11. There is indeed a classical rotation and spreading around Oz, while no rotation occurs around OZ; only spreading is observed around this axis.

Figure 10 illustrates the case of an irrational value of δ, where there are partial revivals for times $t=(m/n)\,T^I_{\rm rev}$ around Oz, and for times $t=(m'/n')\,T^K_{\rm rev}$ where the revivals are around OZ. Note that the concentration of the wave packet for some definite values of α (or γ) has no influence on the other variable γ (or α).

Figure 11 illustrates the case of a rational value of δ, for which there are q^2 clones. The proof that there are q^2 clones if condition (98) holds is rather simple, one applies twice the method of Averbukh and Perelman to linearize the exponential containing k_1^2 and k_2^2 in Eqs. (95) and (96).

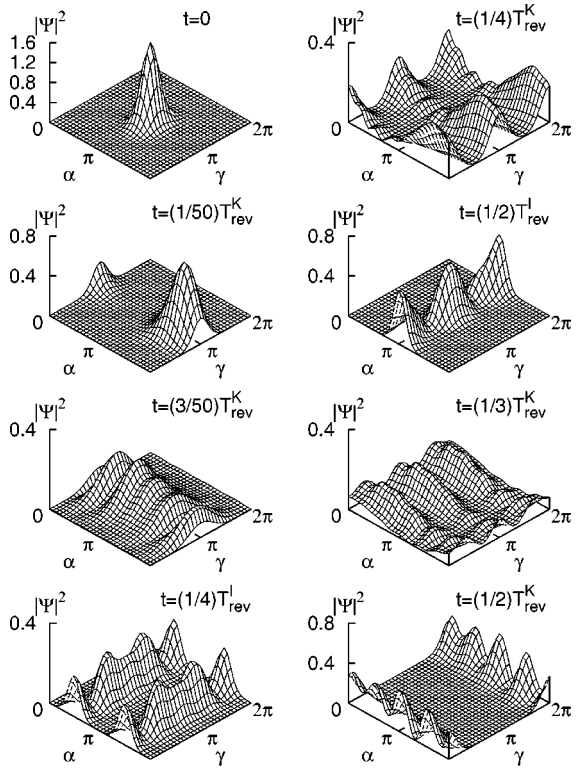

FIG. 10. Time evolution of Janssen's coherent state for an axially symmetric top (95-96) for irrational $\delta=1/\sqrt{3}$ implying $T^I_{\rm rev}=1/\sqrt{3}\,T^K_{\rm rev}\simeq 0.577\,T^K_{\rm rev}$. Shown is the probability density $|\langle\alpha\beta\gamma|\overline{IK}\rangle|^2$ for $\beta=\pi/2$, $\overline{I}=4$, and $\overline{K}=0$. Notice that the vertical scale is not the same in all figures.

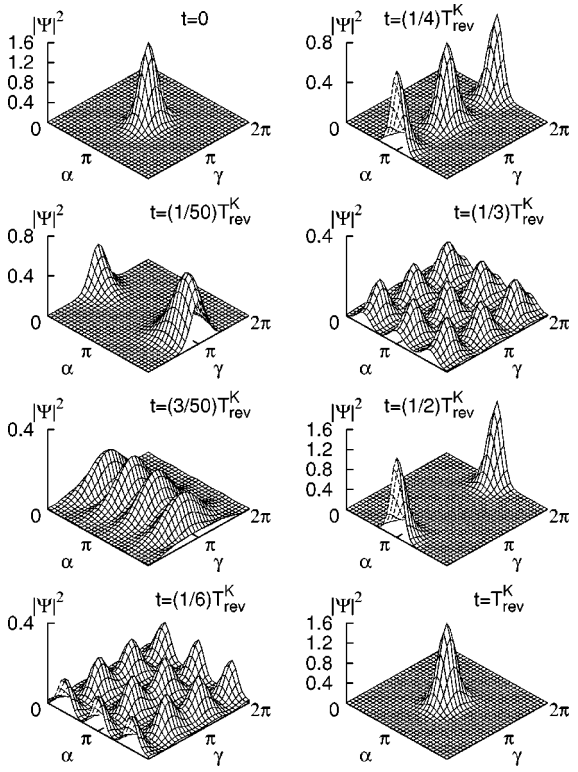

FIG. 11. The same as in Fig. 10 but for rational $\delta=1/2$ implying $T^{I,K}_{\rm rev}=T^K_{\rm rev}=2\,T^I_{\rm rev}$. Clones for times 1/6, 1/3, and $1/2\,T^{I,K}_{\rm rev}$ are clearly visible as well as full revivals. Notice that the vertical scale is not the same in all figures.

Finally we want to stress that the variable β does not play a role in the time evolution. Obviously this is due to our particular choice of axis in Eq. (80). The role played by β for the axial rotor is similar to the role played by θ in the diatomic molecule.

VIII. CONCLUSIONS

We have discussed the time evolution of angular-momentum coherent states that are built from intelligent spin states, but which, as pointed in the Appendix, can be constructed by a simple, purely geometric, generating procedure. The basic ingredients are the three-dimensional Gaussian wave packets of the harmonic oscillator. We have used two of the parameters of the Gaussian to derive an ensemble of coherent states which depends finally on two parameters N and η. The angular distribution of the probability density depends only on N, while the momentum distribution depends both on N and η. The uncertainty relation [Eq. (2)] is valid for all N and η. Such a variety of wave packets does not arise from the previous works on angular-momentum coherent states with bosons. It is, for example, simple to show [36] that there is no place in the work of Atkins and Dobson or Mihailov for wave packets [Eqs. (40) and (41)] which correspond to $\eta=0$. Also, the coefficient α_{jm} defined by Eq. (45) in terms of α_+ and α_- cannot generally be put into the form of Eq. (44), which ensures that b_{IM} is zero if I and M have opposite parities.

In the framework of the scenario of Ref. [1], we have shown that for $\eta=1$ the wave packets spread at $t=(m/n)\,T_{\rm rev}$ into clones. However, the difference between the symmetries for $\eta=0$ and $\eta=1$ necessitates a change in the topology of the fractional wave packets. This change is such that these wave packets can be called mutants due to a certain amount of deformation in their shape. Aronstein and Stroud [2] showed that ''the infinite square well is an ideal system for fractional revivals since all wave functions exhibit fractional revivals of all orders.'' The same statement applies to the case of the diatomic molecule, but is limited to circular wave packets, i.e., to those which contain only $M=I$ partial waves in a convenient axis system. The generation mechanism used in this paper can be extended to shapes different from Gaussian distribution. Clones will always result in this particular condition. For wave packets which contain populations of sublevels $M\neq I$, mutants will appear. All these results hold independently of the realization of the uncertainty condition [Eq. (2)]. For systems where the energy is quadratic in one quantum number, we have shown that the time evolution can exhibit a rich structure of cloning and mutation of fractional revivals. It is a challenging question to find a proper way to excite such wave packets in a rotational band of a molecule or of a deformed nucleus. Let us briefly describe the efforts made under this perspective.

Wave packets with $\eta=0$ or $M=0$ have already been considered several times. In a reference work on Coulomb excitation of nuclei with heavy ions, Broglia and Winther [37] showed that such wave packets are generated in backward scattering. Their population of the excited states of a rotational band with $K=0$ does not coincide with the very sim-

plified expressions (40) and (41). Indeed, interference effects during the excitation process modulate this population to a large extent (Fig. 8; p. 82 of Ref. [37]). However, we have studied the time evolution of such a wave packet, and this will be the subject of a future publication [38].

The authors of Ref. [36] wrote an important analysis on coherent rotational states, completing the work of Ref. [37]. They used the wave $|k,\frac{1}{2}\rangle_i$ of Sec. III, derived from Ref. [26], and considered an extension toward other symmetries like $Sp(2,R)$, $Sp(4,R)$. Time evolution was studied, but only for average values of operators like quadrupole moments. The physical systems considered were the nucleus ^{238}U and the molecule CS_2. The time evolution of expectation values of more general operators for wave packets due to quadratic dependence was studied in Ref. [39]. The operators studied in Ref. [36] have very strict selection rules, and the time evolution reflected there is much poorer than what is exhibited by the full wave packet and by the average values of the more complex observables [39] related to the position. It is, however, clear that all the wave packets considered in Ref. [36] must evolve according to the scenario of Ref. [1], with a very rich sequence of changes of shapes.

Our work comes very near to the spirit of two recent publications devoted to molecular physics. In Ref. [40], the population of a set of rotational states of a molecule by an intense laser was calculated. However, the number of states excited in this way is rather small ($l<4$), the symmetry implies only states with $M=0$, and therefore the WP produced is not concentrated on the sphere as sharply as ours with $N=20$ or 50. In Ref. [41]. Ortigoso studied how to tailor microwave pulses in order to create rotational coherent states for an asymmetric-top molecule, which is built from Radcliffe's intelligent spin states discussed in Sec. II. It is gratifying that such a mechanism, which involves optimal control theory, is possible. However, our demand is more ambitious, since one needs to combine intelligent spin states of different angular momenta in order to achieve a proper angular concentration. In addition, one has to find a mechanism that allows one to change our variable η continuously, i.e., the relative uncertainties in L_x and L_y, in order to explore the total variety of our states as well as of the intelligent spin states. It is indeed interesting that Radcliffe's states were used quite thoroughly, for example, in Refs. [42,43], but our paper points out the fact that a richer structure exists nearby in accordance with older works [19–21]. As stated in the text, we have not used the larger class of intelligent spin states in the case of the diatomic molecule, and we are also conscious that our work on the symmetric top leaves open possibilities of coherent states that have not yet been explored.

It is worth mentioning a very recent paper by Chen and Yeazell [44] concerning an analytical wave-packet design scheme that is able to create the desired Rydberg wave packets and control their dynamics. We believe that we have enriched the examples given in Ref. [10] by pointing out how different the fractional revivals may be.

APPENDIX: CONNECTION BETWEEN THE EXPONENTIAL COHERENT WP AND COHERENT STATES OF THE HARMONIC OSCILLATOR

The exponential WP defined by Eq. (23) can be manufactured from Gaussian wave packets in three dimensions which are coherent states of the harmonic oscillator. Such a general WP, with an average position $\vec{r}_0$ and momentum $\vec{p}_0$, is written as

$$\Psi_G(r,\theta,\phi)=\frac{1}{(2\pi)^{3/4}\sigma^{3/2}}\exp\left[-\frac{(\vec{r}-\vec{r}_0)^2}{2\sigma^2}+i\frac{\vec{p}_0\cdot\vec{r}}{\hbar}\right]. \tag{A1}$$

One gets rid of three unecessary parameters if one chooses the axis in such a way that

$$p_{0z}=0, \quad \vec{r}_0=\hat{x}\,r_0. \tag{A2}$$

With such choices the probability density is

$$|\Psi_G|^2=\left[\frac{1}{(2\pi)^{3/2}\sigma^3}\exp\left(-\frac{r^2+r_0^2}{\sigma^2}\right)\right]\times\exp\left(\frac{2r\,r_0}{\sigma^2}\sin\theta\cos\phi\right). \tag{A3}$$

Apart from a normalization factor, this coincides with Eq. (24) if r and r_0 are both chosen as

$$r=r_0=\sigma\sqrt{N}. \tag{A4}$$

The solid angle $\Omega=4\pi/(4N+1)$ is thus the angle at which the width σ of the density of the Gaussian WP is observed from the center of the sphere of the radius given by Eq. (A4). This choice still leaves two parameters p_{0x} and p_{0y} free. The choices which lead to Eq. (23) are

$$p_{0x}=0, \quad r_0\,p_{0y}=\eta N\hbar. \tag{A5}$$

If one takes the width of the harmonic oscillator $\sigma=\sqrt{\hbar/m\,\omega}$, the value of p_{0y} given in Eq. (A5) leads for $\eta=1$ to

$$p_{0y}=m\,r_0\,\omega. \tag{A6}$$

The coherent state (A1) associated with this value evolves around a circular trajectory in the field of the harmonic oscillator. In the same manner the value $\eta=0$ is associated with a linear trajectory, and the other values of η correspond to elliptic trajectories. In the second case the initial point is either the apogee or perigee of the ellipsis. In this manner more general WP's can also be constructed which start from arbitrary points according to a nonzero value given to p_{x0}. Let us define a parameter ϵ by

$$r_0\,p_{0x}=\epsilon N\hbar. \tag{A7}$$

The exponential WP [Eq. (23)] becomes, in these conditions,

$$\Psi_{\eta,\epsilon}(\theta,\phi)=\sqrt{\frac{N}{2\pi\sinh 2N}}\exp\{N\sin\theta[(1+i\epsilon)\cos\phi+i\eta\sin\phi]\} \tag{A8}$$

and verifies the condition

$$[(1+i\epsilon)L_x+i\eta L_y]\Psi_{\eta,\epsilon}=0. \quad \text{(A9)}$$

The probability density is again given by Eq. (24). However, these more general states do not fulfill condition (2). Indeed, for those states which obey this equation there exists a value of η given by Eq. (7), such that Eq. (6) is obeyed and Eq. (A9) is not. It was then consistent to consider only those WP's with $\epsilon=0$. This result is in accordance with an older result by Rashid [21], and marks a difference between so called *quasi-intelligent spin states* which solve Eq. (A8) but do not satisfy Eq. (2), and the *intelligent spin states* for which $\epsilon=0$.

[1] I. S. Averbukh and N. F. Perelman, Phys. Lett. A **139**, 449 (1989); Usp. Fiz. Nauk. **161**, 41 (1991) [Sov. Phys. Usp. **34**, 572 (1991)].

[2] D. L. Aronstein and C. R. Stroud, Jr., Phys. Rev. A **55**, 4526 (1997).

[3] Z. Dačic–Gaeta and C. R. Stroud, Jr., Phys. Rev. A **42**, 6308 (1990); J. C. Gay, D. Delande, and A. Bommier, *ibid.* **39**, 6587 (1989); M. Nauenberg, *ibid.* **40**, 1133 (1989).

[4] M. Nauenberg, C. R. Stroud, Jr., and J. A. Yeazell, Sci. Am. **270** (6), 24 (1994).

[5] S.D. Boris, S. Brandt, H. D. Dahmen, T. Stroh, and M. L. Larsen, Phys. Rev. A **48**, 2574 (1993).

[6] R. Bluhm and V.A. Kostelecky, Phys. Rev. A **51**, 4767 (1995).

[7] C. Leichtle, I. Sh. Averbukh, and W. P. Schleich, Phys. Rev. Lett. **77**, 3999 (1996); Phys. Rev. A **54**, 5299 (1996).

[8] R. M. Bowman, M. Dantus, and A. H. Zewail, Chem. Phys. Lett. **161**, 297 (1989).

[9] M. J. J. Vrakking, D. M. Villeneuve, and A. Stolow, Phys. Rev. A **54**, R37 (1996).

[10] R. Bluhm, V. A. Kostelecky, and B. Tudose, Phys. Lett. A **222**, 220 (1996).

[11] R. Bluhm, V. A. Kostelecky, and J. A. Porter, Am. J. Phys. **64**, 944 (1996).

[12] G. Alber and P. Zoller, Phys. Rep. **199**, 231 (1991); B. M. Garraway and K. A. Suominen, Rep. Prog. Phys. **58**, 365 (1995).

[13] M. V. Berry and J. Goldberg, Nonlinearity **1**, 1 (1988).

[14] M. V. Berry, Physica D **33**, 26 (1988).

[15] M. V. Berry and S. Klein, J. Mod. Opt. **43**, 2139 (1996).

[16] M. V. Berry, J. Phys. A **29**, 6617 (1996).

[17] J. R. Klauder and B. S. Skagerstam, *Coherent States* (World Scientific, Singapore, 1985).

[18] F. Bloch, Phys. Rev. **70**, 460 (1946); J. M. Radcliffe, J. Phys. A **4**, 313 (1971).

[19] C. Aragone, G. Guerri, S. Salamo, and J. L. Tani, J. Phys. A **7**, L149 (1974).

[20] C. Aragone, E. Chalbaud, and S. Salamo, J. Math. Phys. **417**, 1963 (1976).

[21] M. A. Rashid, J. Math. Phys. **19**, 1391 (1976); **19**, 1397 (1976).

[22] L. Kolodziejczyk and A. Ryter, J. Phys. A **7**, 213 (1974).

[23] G. Vetri, J. Phys. A **8**, L55 (1975).

[24] S. I. Vetchinkin, A. S. Vetchinkin, V. V. Eryomin, and I. M. Umanskii, Chem. Phys. Lett. **215**, 11 (1993).

[25] J. Mostowski, Phys. Lett. A **56**, 369 (1976).

[26] P. W. Atkins and J. C. Dobson, Proc. R. Soc. London, Ser. A **321**, 321 (1971).

[27] J. Schwinger, in *Quantum Theory of Angular Momentum*, edited by L. C. Biedenharn and H. van Dam (Academic, New York, 1965).

[28] D. Janssen, Yad. Fiz. **25** 897 (1977) [Sov. J. Nucl. Phys. **25**, 479 (1977)].

[29] R. Jackiw, J. Math. Phys. **9**, 339 (1968).

[30] R. Bonifacio, D. M. Kim, and M. O. Scully, Phys. Rev. **187**, 441 (1969).

[31] V. V. Mikhailov, Theor. Math. Phys. **15**, 584 (1973); Phys. Lett. A **34**, 343 (1971).

[32] P. Gulshani, Can. J. Phys. **57**, 998 (1979); **25**, 479 (1977).

[33] F. Grossmann, J. M. Rost, and W. P. Schleich, J. Phys. A **30**, L277 (1997).

[34] R. Arvieu and P. Rozmej, Phys. Rev. A **51**, 104 (1995); R. Arvieu, P. Rozmej, and W. Berej, J. Phys. A **30**, 5381 (1997).

[35] A. M. Perelomov, Commun. Math. Phys. **26**, 222 (1972).

[36] L. Fonda, N. Mankoč–Borstnik and M. Rosina, Phys. Rep. **158**, 159 (1988).

[37] R. Broglia and A. Winther, *Heavy Ion Reactions* (Benjamin, New York, 1981).

[38] R. Arvieu and P. Rozmej, e-print quant-ph/9803078.

[39] P. A. Braun and V. I. Savichev, Phys. Rev. A **49**, 1704 (1994).

[40] M. Persico and P. Van Leuven, Z. Phys. D **41**, 139 (1997).

[41] J. Ortigoso, Phys. Rev. A **57**, 4592 (1998).

[42] D. Huber, E. J. Heller, and W. G. Harter, J. Chem. Phys. **87**, 1116 (1987).

[43] C. C. Martens, J. Chem. Phys. **96**, 1870 (1992).

[44] X. Chen and J. A. Yeazell, Phys. Rev. A **57**, R2274 (1998).